

Symmetry Remnants in the Face of Competing Interactions in Nuclei

A. Leviatan^{1,a)} and M. Macek^{2,b)}

¹*Racah Institute of Physics, The Hebrew University, Jerusalem 91904, Israel*

²*Center for Theoretical Physics, Sloane Physics Laboratory, Yale University, New Haven, CT 06520-8120, USA*

^{a)}Corresponding author: ami@phys.huji.ac.il

^{b)}micchal.macek@yale.edu

Abstract. Detailed description of nuclei necessitates model Hamiltonians which break most dynamical symmetries. Nevertheless, generalized notions of partial and quasi dynamical symmetries may still be applicable to selected subsets of states, amidst a complicated environment of other states. We examine such scenarios in the context of nuclear shape-phase transitions.

INTRODUCTION

The inherent simplicity encoded in the pattern of collective states in nuclei, highlights the role of underlying symmetries in explaining their structure. Notable examples are the U(5), SU(3) and O(6) dynamical symmetries of the interacting boson model (IBM) [1], which act as benchmarks for spherical-vibrator, axial-rotor and γ -unstable types of collective motion. Each dynamical symmetry (DS) provides a physically transparent analytic solution and good quantum numbers for all states of the system. The majority of nuclei, however, exhibit strong deviations from these solvable limits. Often, in spite of the required symmetry-breaking terms in the Hamiltonian, some eigenstates appear to obey the symmetry while other states do not. To accommodate such more realistic scenarios, one needs to enlarge the traditional concept of exact symmetries. In the present contribution, we discuss two such generalizations, partial and quasi dynamical symmetries, and show their ability to characterize the remaining regularity amidst a complicated (at times chaotic) environment of other states, a situation encountered in a nuclear shape-phase transition.

PARTIAL AND QUASI DYNAMICAL SYMMETRIES

Partial dynamical symmetry (PDS) corresponds to a situation in which only part of the eigenspectrum is solvable and/or has good symmetry-based quantum numbers [2, 3]. Algorithms for constructing Hamiltonians with PDS are available [3] and empirical evidence for their occurrence in a wide range of nuclei, has been presented [2-8].

PDS reflects the purity of selected eigenstates with respect to a DS basis. Its quantitative measure is based on the concept of Shannon entropy. Consider an eigenfunction of the IBM Hamiltonian, $|L\rangle$, with angular momentum L , and denote by $C_{n_d, \tau, n_\Delta}^{(L)}$ and $C_{(\lambda, \mu), K}^{(L)}$ its expansion coefficients in the U(5) and SU(3) bases, respectively. Here $n_d, \tau, (\lambda, \mu)$ denote U(5), O(5) and SU(3) irreducible representations (irreps) and (n_Δ, K) are multiplicity labels. The U(5) (n_d) and SU(3) $[(\lambda, \mu)]$ probability distributions, $P_{n_d}^{(L)}$ and $P_{(\lambda, \mu)}^{(L)}$, and Shannon entropies, $S_{U5}(L)$ and $S_{SU3}(L)$, are given by

$$P_{n_d}^{(L)} = \sum_{\tau, n_\Delta} |C_{n_d, \tau, n_\Delta}^{(L)}|^2, \quad P_{(\lambda, \mu)}^{(L)} = \sum_K |C_{(\lambda, \mu), K}^{(L)}|^2, \quad S_G(L) = -\frac{1}{\ln D_G} \sum_\alpha P_\alpha^{(L)} \ln P_\alpha^{(L)}, \quad (1)$$

where $[G = U(5), SU(3)]$ and D_G counts the number of possible G -irreps for a given boson-number N and L . $S_G(L)$ vanishes when the considered state is pure with good G -symmetry [$S_G(L) = 0$], and is positive for a mixed state. The maximal value [$S_G(L) = 1$] is obtained when $|L\rangle$ is uniformly spread among the irreps of G , *i.e.*, for $P_G^{(L)} = 1/D_G$. Intermediate values, $0 < S_G(L) < 1$, indicate partial fragmentation of the state $|L\rangle$ in the respective DS basis.

Quasi dynamical symmetry (QDS) corresponds to the situation for which selected eigenstates of a Hamiltonian with broken symmetries, continue to exhibit characteristic properties (*e.g.*, energy and B(E2) ratios) of the closet DS limit [9]. This “apparent” symmetry is due to a coherent mixing of irreps, imprinting an adiabatic motion [10].

In case of SU(3)-QDS, the coherent mixing arises when the SU(3) expansion coefficients, $C_{(\lambda,\mu),K}^{(L)}$, are approximately independent of L for a class of states. Such strong correlations between different L states, signal a common intrinsic structure and the formation of a rotational band. Focusing, for example, on the $L = 0, 2, 4, 6$, members of $K = 0$ bands, given a $L = 0_1^+$ state, among the ensemble of possible states, we associate with it those $L_j > 0$ states which show the maximum correlation, $\max_j \{\pi(0_i, L_j)\}$. A unit value, $\pi(0_i, L_j) = 1$, for the Pearson coefficient implies a perfect correlation. To quantify the amount of coherence (hence of SU(3)-QDS) in the chosen set of states, we consider the product $C_{\text{SU3}}(0_i-6) \equiv \max_j \{\pi(0_i, 2_j)\} \max_k \{\pi(0_i, 4_k)\} \max_\ell \{\pi(0_i, 6_\ell)\}$ [11]. The set of states $\{0_i, 2_j, 4_k, 6_\ell\}$ is considered as comprising a $K = 0$ band with SU(3)-QDS, if $C_{\text{SU3}}(0_i-6) \approx 1$.

ORDER AMIDST CHAOS AND PERSISTING SYMMETRIES

The presence of terms in the Hamiltonian with incompatible (non-commuting) symmetries, has a profound effect on the possible emergence of quantum phase transitions (QPT). The latter are structural changes in the properties of the system induced by a variation of parameters in the Hamiltonian. Such ground state transformations are manifested empirically in nuclei as transitions between different shapes [12]. The competing interactions that drive the QPT can affect dramatically the nature of the dynamics and, in some cases, lead to an intricate interplay of order and chaos [13-15]. Even in such circumstances, generalized symmetries such as PDS and QDS can endure, and be assigned to particular regular multiplets of states which survive amidst a complicated environment of other states [15].

Focusing on the intrinsic dynamics [16] at the critical-point of a first-order QPT between spherical [U(5)] and deformed [SU(3)] shapes, the relevant IBM Hamiltonian can be transcribed in the form [17, 18]

$$\hat{H}_{\text{cri}} = h_2 P_2^\dagger \cdot \tilde{P}_2 \quad , \quad P_{2m}^\dagger = 2d_m^\dagger s^\dagger + \sqrt{7} (d^\dagger d^\dagger)_m^{(2)} \quad , \quad \tilde{P}_{2m} = (-)^m P_{2,-m} \quad , \quad (2)$$

where s^\dagger (d_m^\dagger) are monopole (quadrupole) bosons. \hat{H}_{cri} mixes terms from different DS chains of the IBM, hence is non-integrable. The corresponding classical Hamiltonian, obtained by Glauber coherent states, has a Landau potential with two degenerate spherical and prolate-deformed minima, as shown in Fig. 1.

For $L = 0$, the classical Hamiltonian is two-dimensional and its dynamics can be depicted conveniently via Poincaré surfaces of sections. These (p_x, x) sections in the plane $y = 0$, are shown in the left column of Fig. 1 for representative energies. The dynamics in the region of the deformed minimum ($x \approx 1$) is seen to be robustly regular. The trajectories form a single island and remain regular even at energies far exceeding the barrier height. In contrast, the dynamics in the region of the spherical minimum ($x \approx 0$) shows a change with energy from regularity to chaos, until complete chaoticity is reached near the barrier top. The clear separation between regular and chaotic dynamics, associated with the two minima, persists all the way to the barrier energy, where the two regions just touch. At higher energy, a layer of chaos develops in the deformed region and gradually dominates the surviving regular island.

A quantum analysis is based on Peres lattices [19]. The latter are constructed by plotting the expectation values $x_i \equiv \sqrt{2} \langle i | \hat{n}_d | i \rangle / N$ of the d -boson number operator, versus the energy $E_i = \langle i | \hat{H} | i \rangle$ of the Hamiltonian eigenstates $|i\rangle$. The lattices $\{x_i, E_i\}$ corresponding to regular dynamics display an ordered pattern, while chaotic dynamics leads to disordered meshes of points [19, 20]. The quantity x_i is related to the coordinate x in the classical potential, hence the indicated lattices can distinguish regular from irregular states and associate them with a given region in phase space.

The Peres lattices corresponding to ($N = 50$, $L = 0, 2, 3, 4$) eigenstates of \hat{H}_{cri} are shown in the right column of Fig. 1, overlaid on the classical potential, $V(x, y = 0)$. They disclose regular sequences of states localized within and above the deformed well. They are comprised of rotational states with $L = 0, 2, 4, \dots$ forming regular $K = 0$ bands and sequences $L = 2, 3, 4, \dots$ forming $K = 2$ bands. Additional K -bands (not shown in Fig. 1), corresponding to multiple β and γ vibrations about the deformed shape, can also be identified. Such ordered band-structures persist to energies above the barrier and are not present in the disordered (chaotic) portions of the Peres lattice. At low-energy, in the vicinity of the spherical well, one can also detect multiplets of states with $L = 0$, $L = 2$ and $L = 0, 2, 4$, typical of quadrupole excitations with $n_d = 0, 1, 2$, of a spherical shape.

The nature of the surviving regular sequences of selected states is revealed in a symmetry analysis of their wave functions. The left column of Fig. 2 shows the U(5) n_d -probabilities $P_{n_d}^{(L)}$, Eq. (1), for eigenstates of \hat{H}_{cri} , selected on the basis of having the largest components with $n_d = 0, 1, 2, 3, 4$, within the given L spectra. The states are arranged into panels labeled by ‘ n_d ’ to conform with the structure of the n_d -multiplets of the U(5) DS limit. The U(5) Shannon

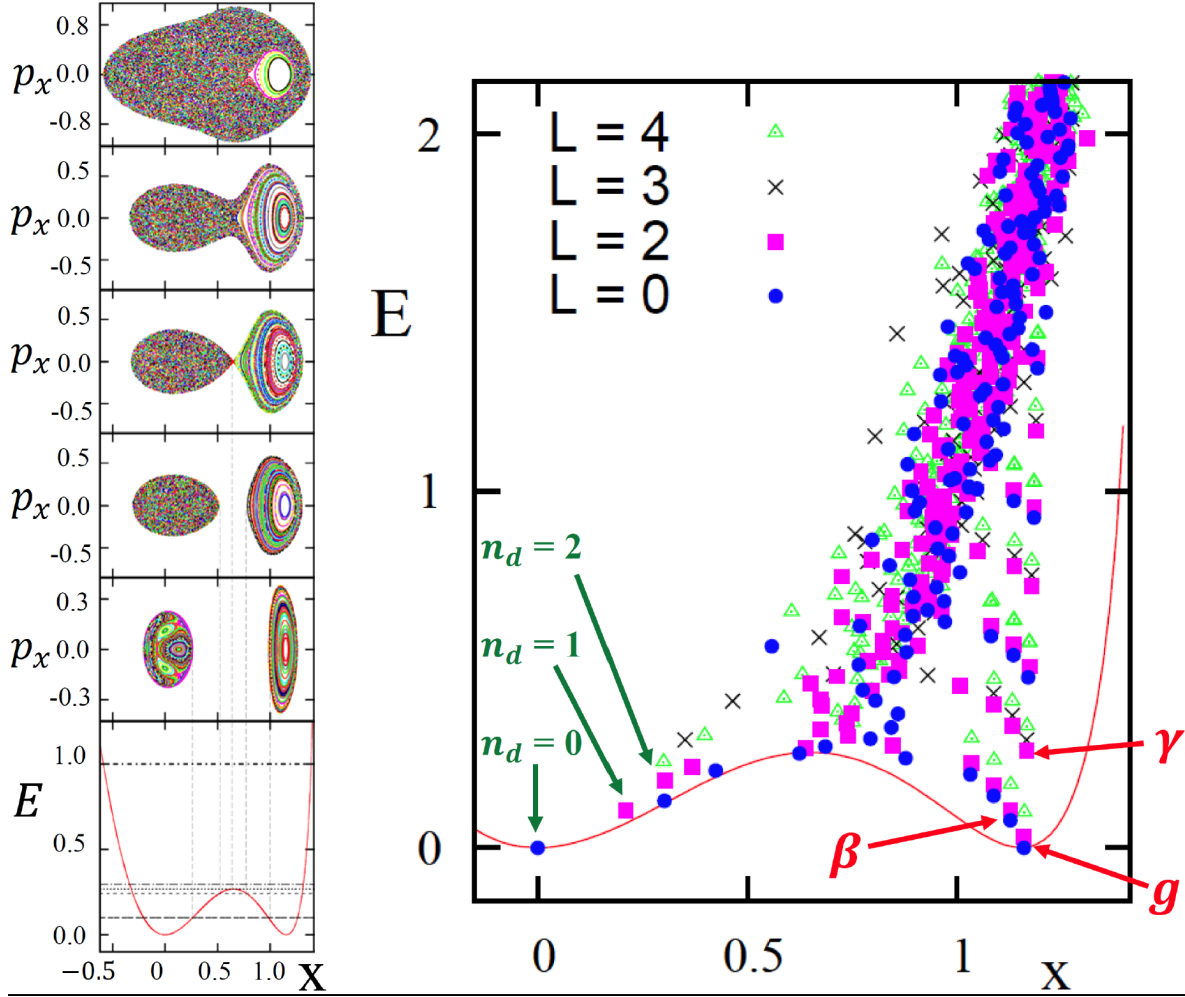


FIGURE 1. Left panel: Poincaré sections for the classical critical-point dynamics (upper five rows) evaluated at five consecutive energies (indicated by horizontal lines in the bottom row on top of the classical potential). Right panel: Peres lattices $\{x_i, E_i\}$ for $L = 0, 2, 3, 4$ and $N = 50$ eigenstates of \hat{H}_{cri} , Eq. (2), overlaid on the classical potential. Regular n_d -multiplets of spherical type of states and a few regular K -bands of deformed type of states, are marked by arrows. Adapted from [15].

entropy $S_{\text{U5}}(L_i)$, Eq. (1), is indicated for representative eigenstates. In particular, the zero-energy $L=0_2^+$ state is seen to be a pure $n_d=0$ state, with $S_{\text{U5}}=0$. It is a solvable eigenstate of \hat{H}_{cri} , exemplifying U(5)-PDS [18]. The state 2_2^+ has a pronounced $n_d=1$ component (96%) and the states ($L=0_4^+, 2_3^+, 4_3^+$) in the third panel, have a pronounced $n_d=2$ component and a low value of $S_{\text{U5}} < 0.15$. All the above states with ‘ $n_d \leq 2$ ’ have a dominant single n_d component, and hence qualify as ‘spherical’ type of states. They are marked by their n_d -values in the Peres lattices of Fig. 1. In contrast, the states in the panels ‘ $n_d = 3$ ’ and ‘ $n_d = 4$ ’ of Fig. 2, are significantly fragmented. A notable exception is the $L = 3_2^+$ state, which is a solvable U(5)-PDS eigenstate with $n_d = 3$ [18]. The existence in the spectrum of specific spherical-type of states with either $P_{n_d}^{(L)} = 1$ [$S_{\text{U5}}(L) = 0$] or $P_{n_d}^{(L)} \approx 1$ [$S_{\text{U5}}(L) \approx 0$], exemplifies the presence of an exact or approximate U(5) PDS at the critical-point.

The states considered in the middle and right columns of Fig. 2 have a different character. They belong to the five lowest regular sequences seen in the Peres lattices of Fig. 1, in the region $x \geq 1$. As shown in the middle column of Fig. 2, they have a broad n_d -distribution $P_{n_d}^{(L_i)}$ and large $S_{\text{U5}}(L) > 0$, hence are qualified as ‘deformed’-type of states, forming rotational bands: $g(K=0)$, $\beta(K=0)$, $\beta^2(K=0)$, $\beta^3(K=0)$ and $\gamma(K=2)$. Each panel in the right column of Fig. 2, depicts the SU(3) (λ, μ) -distribution $P_{(\lambda, \mu)}^{(L_i)}$ for the band members, the SU(3) Shannon entropy $S_{\text{SU3}}(L)$, Eq. (1), for the bandhead state, and the Pearson correlator $C_{\text{SU3}}(0_i-6)$, mentioned above. The ground $g(K=0)$ and $\gamma(K=2)$

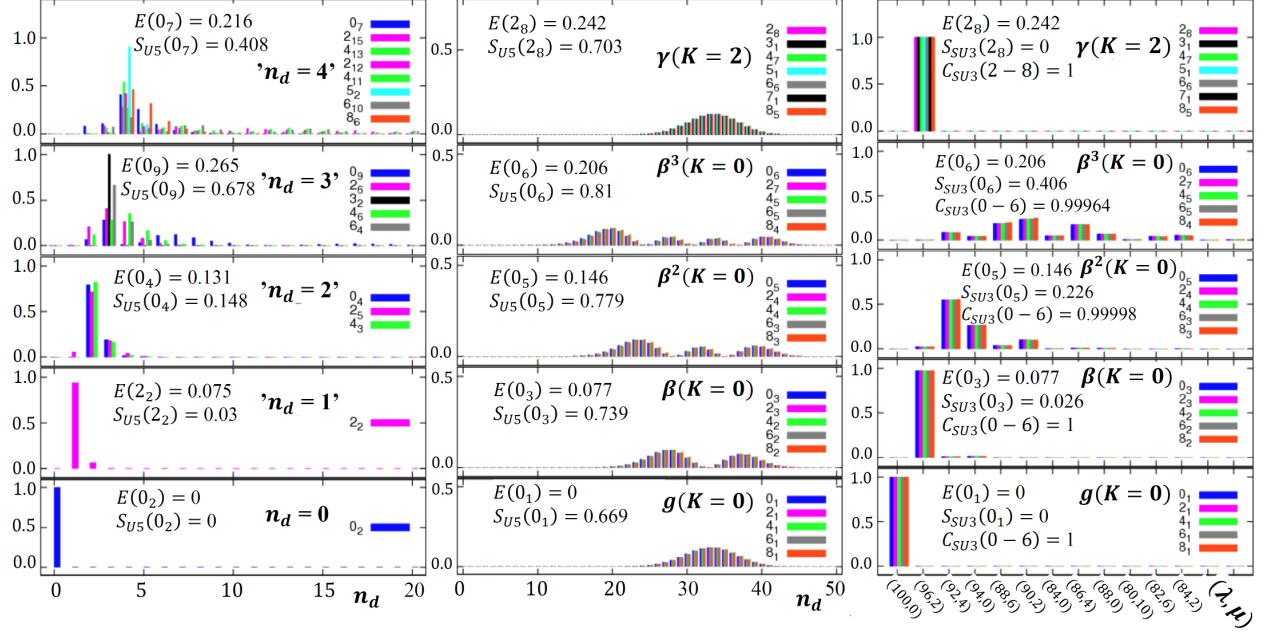


FIGURE 2. U(5) (n_d) and SU(3) $[(\lambda, \mu)]$ decomposition for the regular states shown in Fig. 1. Left column: $P_{n_d}^{(L_i)}$ for spherical type of states arranged in U(5)-like n_d -multiplets. Middle column: $P_{n_d}^{(L_i)}$ for deformed type of states arranged in rotational K -bands. Right column: $P_{(\lambda, \mu)}^{(L_i)}$ for the same deformed type of states. Shannon entropies $S_{U5}(L_i) \approx 0$ and $S_{SU3}(L_i) \approx 0$ signal U(5)-PDS and SU(3)-PDS, respectively. SU(3) Pearson correlator $C_{SU3}(0-6) \approx 1$, signals SU(3)-QDS. Adapted from [15].

bands are pure [$S_{SU3} = 0$] with $(\lambda, \mu) = (2N, 0)$ and $(2N-4, 2)$ SU(3) character, respectively. These are solvable bands of \hat{H}_{cri} and exemplify SU(3)-PDS [18]. The non-solvable K -bands are mixed with respect to SU(3) in a coherent, L -independent manner, hence exemplify SU(3)-QDS. As expected, $C_{SU3}(0_i-6) \approx 1$ for these regular K -bands.

The persistence of regular U(5)-like and SU(3)-like multiplets typifies “emergent simplicity out of complexity” and demonstrates the potential relevance of PDS and QDS in characterizing symmetry remnants in the face of competing interactions in nuclei. This work is supported by the Israel Science Foundation.

REFERENCES

- [1] F. Iachello and A. Arima, *The Interacting Boson Model* (Cambridge Univ. Press, Cambridge, 1987).
- [2] A. Leviatan, Phys. Rev. Lett. **77**, 818 (1996).
- [3] A. Leviatan, Prog. Part. Nucl. Phys. **66**, 93 (2011) and references therein.
- [4] A. Leviatan, J.E. García-Ramos and P. Van Isacker, Phys. Rev. C **87**, 021302(R) (2013).
- [5] R.F. Casten, R.B. Cakirli, K. Blaum and A. Couture, Phys. Rev. Lett. **113**, 112501 (2014).
- [6] P. Van Isacker and S. Heinze, Ann. Phys. (NY) **349**, 73 (2014).
- [7] C. Kremer *et al.*, Phys. Rev. C **89**, 041302(R) (2014).
- [8] P. Van Isacker, J. Jolie, T. Thomas and A. Leviatan, Phys. Rev. C **92**, 011301(R) (2015).
- [9] D. J. Rowe, Phys. Rev. Lett. **93**, 122502 (2004); *ibid.*, Nucl. Phys. A **745**, 47 (2004).
- [10] M. Macek, J. Dobeš, P. Stránský and P. Cejnar, Phys. Rev. Lett. **105**, 072503 (2010).
- [11] M. Macek, J. Dobeš, and P. Cejnar, Phys. Rev. C **82**, 014308 (2010).
- [12] P. Cejnar, J. Jolie and R.F. Casten, Rev. Mod. Phys. **82**, 2155 (2010) and references therein.
- [13] M. Macek and A. Leviatan, Phys. Rev. C **84**, 041302(R) (2011).
- [14] A. Leviatan and M. Macek, Phys. Lett. B **714**, 110 (2012).
- [15] M. Macek and A. Leviatan, Ann. Phys. (NY) **351**, 302 (2014).
- [16] A. Leviatan, Ann. Phys. (NY) **179**, 201 (1987); A. Leviatan and M.W. Kirson, *ibid.* **201**, 13 (1990).
- [17] A. Leviatan, Phys. Rev. C **74**, 051301(R) (2006).
- [18] A. Leviatan, Phys. Rev. Lett. **98**, 242502 (2007).
- [19] A. Peres, Phys. Rev. Lett. **53**, 1711 (1984).
- [20] P. Stránský, P. Hruška and P. Cejnar, Phys. Rev. E **79**, 066201 (2009).